RSC Advances

This is an *Accepted Manuscript*, which has been through the Royal Society of Chemistry peer review process and has been accepted for publication.

Accepted Manuscripts are published online shortly after acceptance, before technical editing, formatting and proof reading. Using this free service, authors can make their results available to the community, in citable form, before we publish the edited article. This *Accepted Manuscript* will be replaced by the edited, formatted and paginated article as soon as this is available.

You can find more information about *Accepted Manuscripts* in the Information for Authors.

Please note that technical editing may introduce minor changes to the text and/or graphics, which may alter content. The journal's standard Terms & Conditions and the Ethical guidelines still apply. In no event shall the Royal Society of Chemistry be held responsible for any errors or omissions in this *Accepted Manuscript* or any consequences arising from the use of any information it contains.

ROYAL SOCIETY OF CHEMISTRY

www.rsc.org/advances

Journal Name

RSCPublishing

ARTICLE

Sintering behavior and thermoelectric properties of $LaCoO_3$ ceramics with Bi_2O_3-B_2O_3-SiO_2 as a sintering aid

Cite this: DOI: 10.1039/x0xx00000x

Jiao Han, Ying Song*, Xue Liu, and Fuping Wang*

Received Xth XXXXXXXXX 20XX
Accepted Xth XXXXXXXXX 20XX

DOI: 10.1039/x0xx00000x

www.rsc.org/

Recently, $LaCoO_3$ has received increasing attention as a promising thermoelectric oxide. However, its sintering temperature is too high from the practical point of view. This study investigated the effect of Bi_2O_3-B_2O_3-SiO_2 (*BBS*) as a sintering aid on the low-temperature sintering behaviors, microstructures and thermoelectric properties of $LaCoO_3$ ceramics. The XRD results revealed that the $LaCoO_3$ ceramics with 1~3 wt.% *BBS* could form a single crystalline phase without visible secondary phases. The sintering temperature of $LaCoO_3$ ceramics was reduced remarkably from 1200 °C to 950 °C by adding 3 wt.% *BBS*, with a relative density higher than 95%. The process of densification and the appearance of rod-like grain in $LaCoO_3$ with *BBS* aids were observed by SEM. Meanwhile, the thermoelectric properties of $LaCoO_3$ ceramics were strongly dependent on the densification and microstructures. For the samples sintered at 1050 °C, the electrical conductivity increased significantly with the increase of *BBS* content (*x*, wt.%) up to x = 2.0, and the Seebeck coefficient were almost the same when the test temperatures were higher than 200 °C. Moreover, the sample with x=2.0 had the optimum thermoelectric properties with ZT=0.05 at 400 °C, which was about 66.7% higher than that of pure $LaCoO_3$ ceramics sintered at 1200 °C, indicating that the addition of *BBS* could effectively promote the densification and further improve thermoelectric properties of $LaCoO_3$ ceramics without using complicated processes.

Introduction

Thermoelectric (TE) materials have been attracting much attention in recent years because of their great application potential to transfer energy between heat and electricity without mechanical device. The efficiency of a TE material is usually described by the dimensionless figure of merit *ZT*, defined as $S^2\sigma T/k$, where *S*, *T*, σ, and *k* are Seebeck coefficient, absolute temperature, electrical conductivity, and thermal conductivity, respectively. Therefore, a good TE material should have a high electrical conductivity σ, a high Seebeck coefficient *S*, and a low thermal conductivity *k*.

Most thermoelectric oxides have been investigated so far, including $CaMnO_3$, $SrTiO_3$ and $LaCoO_3$. $LaCoO_3$ system with a perovskite structure has large Seebeck coefficient (*S*) of 600 $\mu V \cdot K^{-1}$ in the vicinity of room temperature[1], however, its TE properties are still very low for practical application[2]. Recently, many strategies to enhance the thermoelectric performance have been developed in the $LaCoO_3$ system, such as La-site or Co-site substitutions[3-7], and microstructure control[8,9]. For example, Vulchev et al.[6] evaluated the effect of double substitution with Ni and Fe on the thermoelectric efficiency of $LaCoO_3$. They reported that the composition with $LaCo_{0.8}Ni_{0.1}Fe_{0.1}O_3$ exhibited the best thermoelectric activity with ZT = 0.16 at room temperature mainly due to the decrease in the thermal conductivity (*k*) induced by the synergic effect of the double substitution. Li et al.[8] designed a core-shell structure of $LaCoO_3$ ceramics to enhance its electrical conductivity while keeping low thermal conductivity, in which the Ni-doped $LaCoO_3$ with high Seebeck coefficient was selected as the interior, and the Ni and Sr co-doped $LaCoO_3$ with high electrical conductivity was used as the surface coating layer. They found that electrical and thermal transport properties could be separately controlled according to the requirement for enhancing thermoelectric properties by introducing the composite microstructure. Wang et al.[10] reported that the creation of vacancies in La/O sites could effectively reduce the thermal conductivity by strong point-defect scattering, thus leading to an increase in the dimensionless figure of merit *ZT* of $La_{1-x}CoO_{3-y}$, which provided an effective pathway for the design of better thermoelectric oxides. In addition, our previous work improved the thermoelectric properties of $LaCoO_3$ ceramics by the combination of the ultrafine microstructure controlled by the low-temperature liquid-phase sintering and Cu^{2+} substitution provided by the B_2O_3-CuO addition[9]. The results showed that the sintering temperature of $LaCoO_3$ ceramics could be reduced significantly from 1200 °C to 1000 °C by using B_2O_3-CuO additions and the ZT_{max}= 0.073 was obtained at 100 °C, which was about 1.5 time higher than that

RSC Advances Accepted Manuscript

of pure $LaCoO_3$ sintered at 1200 °C. However, the optimization of the thermoelectric performance and the reduction of the sintering temperature are still challenges for the $LaCoO_3$ system. Thus, more sintering aids are needed to investigate in order to control the complicated microstructure with grain boundary phases and the reduced grain size, which could lower the lattice thermal conductivity by the enhanced boundaries phonon scattering, while the thermoelectric power factor ($P=S^2\sigma$) is not affected.

Bi_2O_3-B_2O_3-SiO_2 (*BBS*) eutectic with glass transition temperature around 300 °C[11] is a kind of novel sintering aid used in the field of low-temperature co-fired ceramics[12]. In this study, the sintering behavior and the thermoelectric properties of $LaCoO_3$ ceramic were investigated with an emphasis on the influence of *BBS* in relation to the relative density, microstructure and thermoelectric properties of the sintered ceramics.

Experimental procedures

Materials Synthesis

$LaCoO_3$ powders were prepared starting from $La(NO_3)_3\ 6H_2O$ and $Co(CH_3COO)_2{\cdot}4H_2O$ through the polyacrylamide gel method as reported in our previous work[9]. BBS additive was prepared by milling a mix of Bi_2O_3, B_2O_3 and SiO_2 with a molar ratio of 6:3:1 in a planetary agitator, and then added to the 600 °C pre-calcinated $LaCoO_3$ powder with different contents *x* (wt. %, *x* =0, 1.5, 2.0, 3.0). The mixed powders were milled with absolute ethyl alcohol for 24 h in a planetary agitator. After being dried and grinded, the powders were granulated with a 4 wt. % polyvinyl alcohol (*PVA*) solution and then sieved through a 60-mesh. Finally, the mixed powers were compacted into disk-shaped specimens of 20 mm in diameter and 3~4 mm in thickness under the pressure of about 100 MPa. Sintering of the pellets was carried out in air at temperatures ranging from 950 °C to 1150 °C for 6 h with a heating rate of 5 °C/min and being cooled inside the furnace to room temperature.

Characterization

The X-ray diffraction XRD (Rigaku D/MAX-2550V) of the sample was measured using a standard diffract meter with Cu *Kα* radiation as an X-ray source. Densities of the samples were measured by the Archimedes method. The morphology was studied by observing the fractured cross section of the samples using a field emission scanning electron microscope (Camscan, MX2600FE).

Thermoelectric properties were measured along a specimen surface perpendicular to the pressing direction. The electrical conductivity and Seebeck coefficient were recorded simultaneously as a function of temperature from 50 °C to 500 °C in He atmosphere by using a standard four-probe method on ULVAC ZEM-3 system. Thermal conductivity was calculated from bulk density, specific heat, and thermal diffusivity measured by a laser flash method (Netzsch, LFA457, Germany).

Results and discussion

Fig.1 shows the relative densities of the $LaCoO_3$ ceramics sintered at different temperatures as function of the Bi_2O_3-B_2O_3-SiO_2 (*BBS*) contents *x*. The relative densities of all samples increase with the increasing sintering temperatures and *BBS* contents. It is noted that the relative density of the sample with $x = 0$ is still below 85% even the sintering temperature is up to 1150 ℃. However, the relative density of the samples sintered at 950 ℃ increases from 76.3% to 95.8% as *x* rises from 0 to 3.0, and the samples sintered at 1000 ~1150 ℃ show the similar trend. It could also be seen that the relative densities of the samples with $x \geq 2.0$ sintered above 1000 °C are around 96~98%, approaching that of pure $LaCoO_3$ (~97%) sintered at 1200 ℃ in our previous study[9]. This suggests an unusually fast densification process due to the formation of some BBS liquid phases in the $LaCoO_3$ matrix [13], which could enhance mass transfer and speed up the grain growth. Thus, the densification temperature of $LaCoO_3$ ceramics with *x* =3.0 can be reduced from 1200 ℃ to 950 ℃ by the liquid phase sintering.

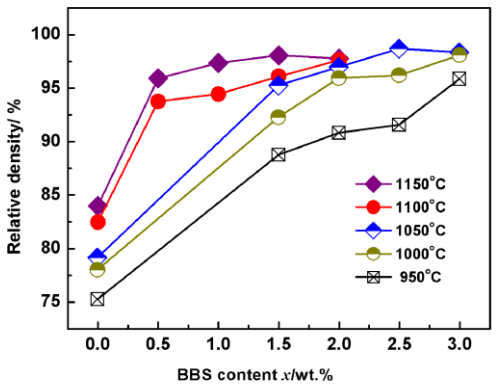

Fig.1 Relative densities of $LaCoO_3$ ceramics sintered at different temperatures as function of the content of *BBS* additives

The composition and crystallinity of the fabricated materials were checked with XRD technology. As shown in Fig. 2 for the samples sintered at 1050 °C, there are three major diffraction peaks at 32.88 º, 33.30 º and 47.50 º observed for the $LaCoO_3$ crystals, which can be assigned to (110), (104) and (024) lattice planes of $LaCoO_3$ (JCPDS card No.48-0123), respectively. It is determined that there is a single crystalline phase of $LaCoO_3$ presenting in all the specimens, without any clear evidence of secondary phases. This may be attributed to the low content of *BBS* in $LaCoO_3$ ceramics, which is difficult to be detected by XRD. Moreover, the XRD results of the other samples sintered at 950 °C or 1150 °C (not shown here) are consistent with what mentioned above.

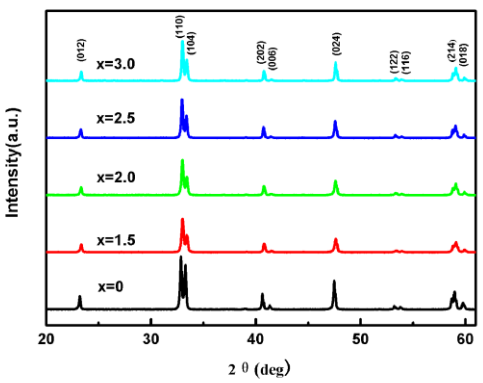

Fig.2 XRD patterns of $LaCoO_3$ ceramics with different amount of *BBS* additives sintered at 1050 ℃

RSC Advances Accepted Manuscript

This journal is © The Royal Society of Chemistry 2012

Fig. 3 displays the SEM micrographs of the fresh fractures for the samples with x = 2.0 and x = 3.0 sintered at temperatures from 950~1150 ℃. As shown in Fig.3(a) and 3(b), the microstructure of the samples sintered at 950 ℃ indicates that the grains size of the sample with x =2.0 are around 1.0 μm, and there are many pores existing due to an insufficient densification. With the increasing of *BBS* up to x=3.0, it can be seen that the microstructure is more dense and the grain size becomes larger as well from ~1.0 μm for x=2.0 to ~2 μm for x=3.0. This grain growth and morphology change may originate from the presence of the liquid phase formed by *BBS*, which speeds up the particle rearrangement behavior at the early period of sintering and the mass transportation at the middle period during the sintering process[14]. However, the samples sintered at 1050 °C have the different trend as showed in Fig. 3(c) and 3(d). The microstructure became denser while the grains size was not larger with the increase of x from x=2.0 to x=3.0. This can be explained by a simple power law[15] as follows:

$$G^n - G_0^n = Kt \quad (1)$$

where G_0 is the initial grain size after the liquid formation transients, G is the grain size during liquid phase sintering, and t is the sintering time, n is near to 3， K is the grain growth rate constant. K is normalized to the Ostwald ripening model where the grain growth rate constant is given as[16]

$$K = \frac{64}{9}\frac{D_S C \Omega \gamma_{SL}}{RT} \quad (2)$$

where D_S is the solid diffusivity in the liquid, C is the solubility of the solid in the liquid, Ω is the solid molar volume, γ_{SL} is the solid-liquid interface energy, R is the gas constant, and T is the absolute temperature. The thermal stability of $LaCoO_3$ ceramics is excellent because $LaCoO_3$ is a high melting point compound. The changes of D_S、C、Ω、γ_{SL} are subtle with small temperature difference and a little amount of liquid phase so that the grain growth rate constant K is mainly depended on temperature. For the samples sintered at 950 °C and 1050 °C, the sample sintered at 950 °C has larger K compared to that sintered at 1050 °C according to Eq. (2). Simultaneously, the sintering time t is consistent. Thus, the increase of grain size is more obvious for the samples sintered at 950 °C according to Eq. (1).

Moreover, some rod-like grains could be observed from the circled area amplified in the inset of Fig. 3(d). The reasons may be as follows: The *BBS* phase is around the grain boundary and the small grains of $LaCoO_3$ are dissolved away from contact points between adjacent solid particles separated by *BBS*, leading to the rod-like grain growth. Nevertheless, this is an open issue yet and needs further clarification. In addition, all $LaCoO_3$ samples with *BBS* addition show inter-granular fracture morphology, indicating that the grain boundaries are mechanically weaker than the grains. This is quite different with that of $LaCoO_3$ samples with B_2O_3-CuO addition in our previous work[9].

Fig. 3(a), 3(c), 3(e) and 3(f) indicate the grain morphology of specimens with x=2.0 sintered at 950 °C, 1050°C, 1100 °C and 1150 °C, respectively. Obvious grain growth and reduction in porosity are observed for the samples with the increasing sintering temperatures. However, some pores could be found on the surface of grains, especially for the samples sintered at 1100 °C and 1150 °C, originating from the volatility of *BBS* at higher temperatures.

Fig.4 shows the temperature dependence of the electrical conductivity (a), Seebeck coefficient (b), and power factor (c) for all samples sintered at 1050 °C with different *BBS* contents. Data for pure $LaCoO_3$ sample sintered at 1200 °C in our previous study[9], which is abbreviated as $LaCoO_3$(C), are given by dashed lines for comparison. As shown in Fig.4 (a), σ for all the samples increases with the measuring temperature, being indicative of semiconducting behavior. There is an obvious σ transition at about 200 °C for all samples, i.e. σ increases slightly with temperatures from 50 °C to 200 °C, however, σ increases remarkably until reaching maximum when temperature is 500 °C. This mutation of different temperature section suggests a different conductive mechanism, which is related to the temperature induced spin-state transition of Co^{3+} [17,18]. In addition, the σ increases obviously with increasing x up to x=2.0, and then decreases after a maximum value. For example, σ at 500 °C increases remarkably from about 531.21 $S \cdot cm^{-1}$ for x=0 to ~1046.5 $S \cdot cm^{-1}$ for x=2.0, which is about 11% higher than that of $LaCoO_3$(C), and then to ~874.5 $S \cdot cm^{-1}$ for x=3.0. For the samples sintered at 1050 °C with x=0~2.0, the porosity of the samples decreases gradually due to the formation of liquid phase and the increases of grain sizes with increasing x, resulting in the enhancement of σ. For the sample with x =3.0, whose relative density is around 98%, the decrease of σ could be related to the segregation of thick *BBS* phase with low electrical conductivity at grain boundaries and appearance of rod-like grains around boundaries.

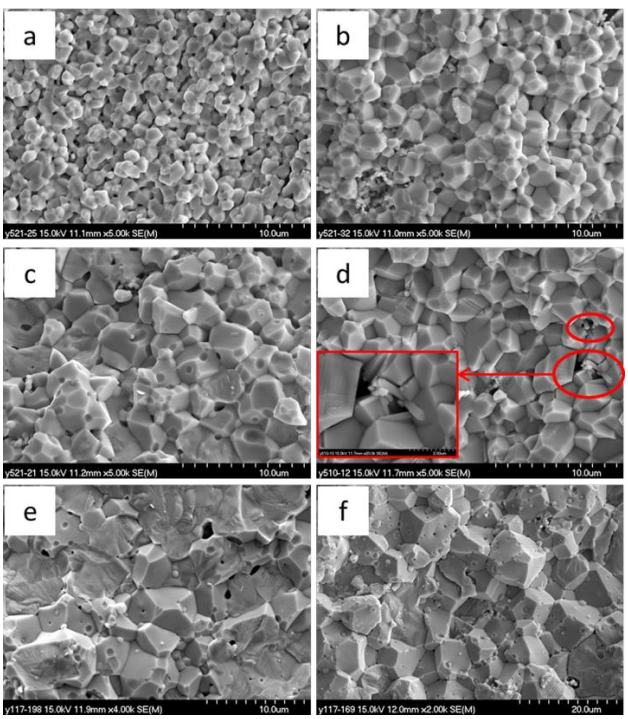

Fig.3 SEM photographs of the fractured surface of the $LaCoO_3$ ceramics with different *BBS* contents and sintering temperature. (a) x=2.0, 950 °C (b) x=3.0, 950 °C (c) x=2.0, 1050 °C (d) x=3.0, 1050 °C (e) x=2.0, 1100 °C (f) x=2.0, 1150 °C. The inset of Fig. 3(d) shows amplified rod-like grain structure of the circled area.

Furthermore, the plots of σ tested at 400 °C versus *BBS* contents x for the samples sintered at different temperatures are

RSC Advances Accepted Manuscript

presented in the inset of Fig. 4(a). For the samples with x=0, the σ increases obviously from 117.2 $S \cdot cm^{-1}$ to 501.8 $S \cdot cm^{-1}$ with the increasing of sintering temperature from 950 °C to 1100 °C, which is mainly attributed to the enhancement of relative density. For the samples with x =1.5 and x = 2.0, the σ increases with the increasing of sintering temperature up to 1050 °C and then decreases slightly. This may be attributed to the carrier scattering caused by the pores observed on the surface of grain sintered at 1100 °C and 1150 °C as shown in Fig. 3(e) and 3(f). For the samples with x=3.0, the σ decreases with increasing sintering temperatures due to the volatilization of *BBS* and appearance of rod-like grain as shown in Fig. 3(d), which may inhibit carrier transmission or change transmission path, leading to a reduction of the electrical conductivity.

All the samples display a positive Seebeck coefficient at the measured temperature ranging from 50 °C to 500 °C as shown in Fig. 4(b), being indicative of p-type conduction with holes as the major carriers. As temperature increases from 50 °C to 200 °C, the Seebeck coefficient of samples decreases significantly, then it decreases slowly to ~30 $\mu V \cdot K^{-1}$ as temperature increases further to 500 °C. This temperature behavior of S can be explained by the modified Heikes' equation as discussed in previous studies[19-21], which indicates that the Seebeck coefficient depends on the degeneration of electronic states of Co^{3+} and Co^{4+} ions as well as the ratio between them. In addition, as temperature increases from 50 °C to 200 °C, S of pure $LaCoO_3$ ($LaCoO_3$(C) or x=0) is higher than that of samples with BBS due to the potential barrier to filter low energy carriers[22], while they are close at temperature ranging from 200 °C to 500 °C because the holes produced by the thermally activated low-spin Co^{4+} from low-spin Co^{3+} are saturated[23]. Moreover, the bar chart of S at 400 °C versus *BBS* content x for the samples sintered at different temperatures are presented in the inset of Fig. 4(b). It could be seen that the influence of sintering temperature and BBS content for S tested at 400 °C is unobvious.

Combining the electrical conductivity and Seebeck coefficient, temperature dependence of the power factor ($P=S^2\sigma$) for the samples sintered at 1050 °C are calculated and shown in Fig. 4(c). It can be seen that the P of all the samples increases with elevated temperature from 50 °C to 400 °C, and then decreases gradually. For the samples with BBS addition, P increases with x up to x=2.0 and then decreases as x =3.0 due to the change of σ. The highest P is 1.15×10^{-4} W m^{-1} K^{-2} measured at 400 °C for the sample with x =2.0, which is about 94 % higher than that of sample with x=0 sintered at 1050 °C and 21% higher than that of $LaCoO_3$(C). Furthermore, the change trend of P at 400 °C versus *BBS* content x for the samples sintered at different temperatures is in accord with that of σ, as shown in the inset of Fig. 4(c).

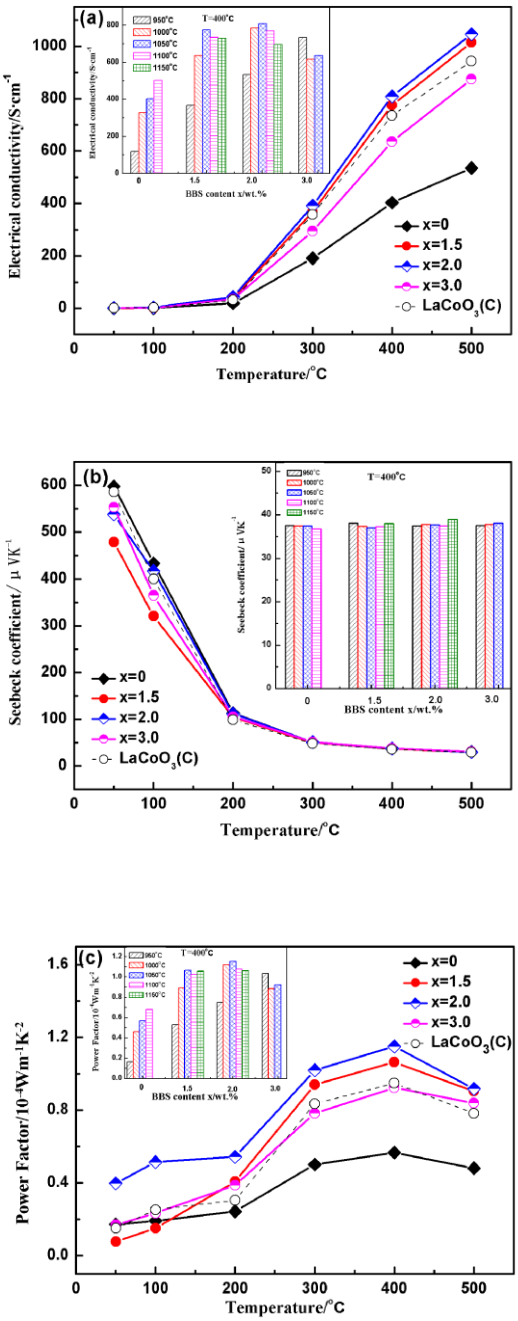

Fig. 4 Temperature dependences of electrical conductivity σ(a), Seebeck coefficient S(b) and power factor P(c) of the $LaCoO_3$ ceramics sintered at 1050 °C in the temperature range from 50 to 500 °C. The inset shows the plots of σ/S/P versus BBS contents x for the samples sintered at different temperatures.

Fig.5 presents the temperature dependence of thermal conductivity (a) and ZT (b) for $LaCoO_3$ with x=2.0 and 3.0 sintered at 950 °C, 1050 °C and 1150 °C, compared with $LaCoO_3$(C). All the samples shown in Fig.5 have high relative densities around 95-97% so that the comparisons of k and ZT are reliable and intrinsically meaning. The data of the $LaCoO_3$(C) are also shown by a dashed line for comparison. As shown in Fig. 5(a), the thermal conductivity k of the samples

RSC Advances Accepted Manuscript

This journal is © The Royal Society of Chemistry 2012

shows an increasing trend as temperature increases, which contributes to the increase in heat transport by the conductive carrier at higher temperatures. In addition, over the measured temperature range, *k* decreases with the decrease of the sintering temperatures and *k* for samples with *BBS* sintered in the range from 950 °C to 1150 °C is much lower than that of $LaCoO_3$(C), which is attributed to the enhanced phonon scattering by the complicated microstructure with *BBS* grain boundary phases and the reduced grain size caused by the low temperature sintering.

In Fig. 5(b), it could be seen that the *ZT* of all the samples increases with elevated temperature up to 400 °C, and then decreases gradually. The *ZT* of the samples with *BBS* is much higher than that of $LaCoO_3$(C), which originates from the higher *k* of $LaCoO_3$(C). The maximum *ZT* value reaches 0.05 at 400 °C for the sample with x =2.0 sintered at 1050 °C, which is about 24% higher than that of sample with x =3.0 sintered at 950 °C and 67% higher than that of $LaCoO_3$(C) sintered at 1200 °C. Note that the $LaCoO_3$ ceramics with *BBS* sintering aid, like pure $LaCoO_3$ ceramics, have the maximum *ZT* value at 400 °C. However, most of the La-site or Co-site substituted $LaCoO_3$ ceramics and the $LaCoO_3$ ceramics with B_2O_3-CuO addition[9] have the maximum *ZT* value around 100 °C. The different temperature dependence of *ZT* is useful for the design of functional graded thermoelectric materials. Though the maximum *ZT* of the samples with *BBS* addition is a little lower than the *ZT* value at 400 °C of the $LaCoO_3$ ceramics with B_2O_3-CuO addition[9], it is much higher than most of the reported *ZT* value at 400 °C, such as those reported by Li et al.[24] for $LaCo_{0.85}Cu_{0.15}O_{3-\delta}$ (*ZT*=0.022 at 400 °C) and reported by Kun et al.[25] for $La_{0.99}Ba_{0.03}CoO_3$ (*ZT*=0.025 at 400 °C). Therefore, the low temperature sintering strategy opens a new possibility with low cost for improving the thermoelectric performance of oxides. Some optimizations of composition and the added amount for sintering aids are needed to obtain dense ultra-fine or nano-structure thermoelectric oxide ceramics at lower sintering temperatures, which may have the enhanced power factor and the reduction of the thermal conductivity due to the enhancement of scattering effects originating from the higher grain boundary density.

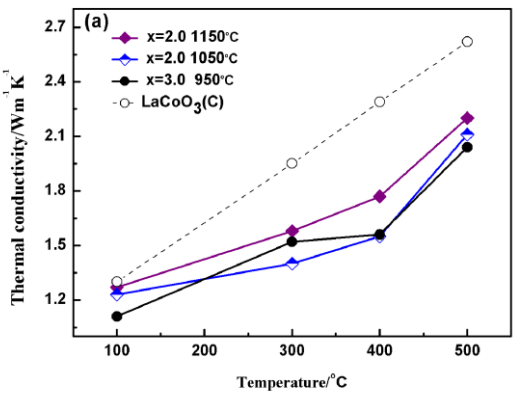

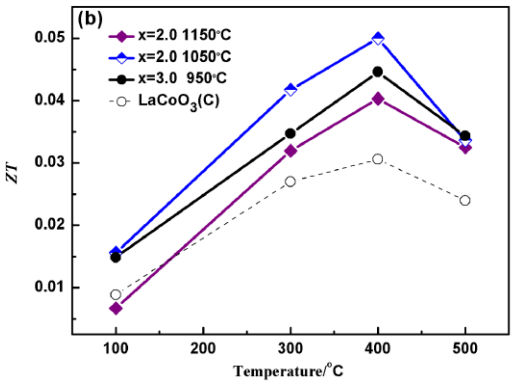

Fig. 5 Temperature dependences of *k*(a) and *ZT*(b) for $LaCoO_3$ sintered at different temperatures.

Conclusions

The low-temperature sintering behaviors, microstructures and thermoelectric properties of the $LaCoO_3$ ceramics with Bi_2O_3-B_2O_3-SiO_2 addition were investigated in the temperature range from 50 °C to 500 °C in this study. The sintering temperature of $LaCoO_3$ ceramics was reduced remarkably from 1200 °C to 950 °C by adding BBS aids (x =3.0), with a relative density higher than 95%, originating from the formation of a low-melting-point liquid phase of *BBS*. The addition of *BBS* in $LaCoO_3$ ceramics improved the electrical conductivity due to the increase of densification while decreased the thermal conductivity because of the enhanced phonon scattering by the complicated microstructure with *BBS* grain boundary phases and the reduced grain size caused by the low temperature sintering. For the samples sintered at 1050 °C, the electrical conductivity increased significantly with the increase of BBS content up to x = 2.0, and the Seebeck coefficient were almost the same when the test temperatures were higher than 200 °C. The sample with x=2.0 had the maximum *ZT*=0.05 at 400 °C, which was about 66.7% higher than that of $LaCoO_3$(C) ceramics sintered at 1200 °C, indicating that the low temperature sintering strategy provides a low cost and facile approach to improve the sinterability and thermoelectric performance of oxides.

Acknowledgements

This work was supported by the National Nature Science Foundation of China (grant No. 50772026).

Notes and references

School of Chemical Engineering and Technology, Harbin Institute of Technology, Harbin 150001, China.
** The corresponding authors, songy@hit.edu.cn (Y.Song); fpwang@hit.edu.cn (F.P. Wang) .*

1 S. Hebert, D. Flahaut, C. Martin, S. Lemonnier, J. Noudem, C. Goupil, A. Maignan and J. Hejtmanek, *Prog. Solid State Chem*, 2007, 35, 457.
2 Z. Jirák, J. Hejtmánek, K. Knížek and M. Veverka, *Phys. Rev. B*, 2008, 78, 014432.
3 H. Kozuka, K. Yamagiwa, K. Ohbayashi and K. Koumoto, *J. Mater. Chem*, 2012, 22,11003.
4 K. Berggold, M. Kriener, C. Zobel, A. Reichl, M. Reuther, R. Müller, A. Freimuth and T. Lorenz, *Phys. Rev. B*, 2005 ,72, 155116.

RSC Advances Accepted Manuscript

5 H. C. Wang, C. L. Wang, W. B. Su, J. Liu, H. Peng, J.L. Zhang, M.L. Zhao, J.C. Li, N. Yin and L.M. Mei, *J. Alloys Compd*, 2009, 486, 693.
6 V. Vulchev, L. Vassilev, S. Harizanova, M. Khristov, E. Zhecheva and R. Stoyanova, *J. Phys. Chem. C*, 2012, 116, 13507.
7 S. Shafeie, J. Grins, S. Y. Istomin, A. A. Gippius, L. Karvonen, S. Populoh, A. Weidenkaff, J. Kohler and G. Svensson, *J. Mater. Chem*, 2012, 22, 16269.
8 F. Li and J. F. Li, *J. Am. Ceram. Soc*, 2012, 95, 3562.
9 Y. Song, Q. Sun, Y. Lu, X. Liu and F. P. Wang, *J. Alloys Compd*, 2012, 536, 150.
10 Y. Wang, F. Li, L. Xu, Y. Sui, X. J. Wang, W. H. Su and X. Y. Liu, *Inorg. Chem*, 2011, 50, 4412.
11 X.M. Zhu, C.L. Mai and M.Y. Li, *J. Non-Cryst. Solids*, 2014, 388 , 55.
12 Y. L. Liu, H. W. Zhang, D. M. Chen and Q. Y. Wen, *J. Appl. Phys*, 2010, 107, 09A507.
13 B. S. Kim, E. S. Lim, J. H. Lee and J. J. Kim, J EUR CERAM SOC, 2007, 27, 819.
14 C. Zhang, R. Zuo, Q. Sun, Z. W. Hu and J. J. Zhang , *Ceram. Int*, 2013, 39, 5675.
15 R. M. German, P. Suri and S. J. Park, *J. Mater. Sci*, 2009, 44, 1.
16 I. M. Lifshitz and V. V. Slyozov. *J. Phys. Chem. Solids*, 1961, 19, 35.
17 Y. Tokura, Y. Okimoto, S. Yamaguchi, H. Taniguchi, T. Kimura and H. Takagi, *Phys. Rev. B*, 1998,58, 1699.
18 I. Terasaki, S. Shibasaki, S. Yoshida and W. Kobayashi, *Materials*, 2010, 3, 786.
19 W. Koshibae, K. Tsutsui and S Maekawa, *Phys. Rev. B*, 2000, 62, 6869.
20 A. Maignan, D. Flahaut and S. Hebert, *Eur. Phys. J. B*, 2004, 39, 145.
21 A.J. Zhou, T.J. Zhu, X.B. Zhao and H.Y. Chen, *E. Muller, J. Alloys Compd*, 2008, 449, 105.
22 K. Kishimoto, M. Tsukamoto and T. Koyanagi, *J. Appl. Phys*, 2002, 92, 5331.
23 A.J. Zhou, T.J. Zhu and X.B. Zhao, *J. Mater. Sci*, 2008, 43, 1520.
24 F. Li, J. F. Li, J. H. Li and F. Z. Yao, *Phys. Chem. Chem. Phys*, 2012, 14, 12213.
25 R. Kun, S. Populoh, L. Karvonen, J. Gumbert, A. Weidenkaff and M. Busse, *J. Alloy. Compd*, 2013, 579, 147.

RSC Advances Accepted Manuscript

 This journal is © The Royal Society of Chemistry 2012